Front. Chem. China 2009, 4(3): 269–277
DOI 10.1007/s11458-009-0087-7

RESEARCH ARTICLE

Dye-sensitized solar cells based on bisindolylmaleimide derivatives

Qiong ZHANG[1,2], Zhijun NING (✉)[1], Hongcui PEI[1] and Wenjun WU[1]

Three organic dyes based on bisindolylmaleimide derivatives (I1, I2 and I3) were synthesized and investigated as sensitizers for the application in nanocrystalline TiO_2 solar cells. The indole group, maleimide group and carboxylic group functioned as electron donor, acceptor and anchoring group, respectively. Solar-to-electrical energy conversion efficiencies under simulated amplitude-modulated 1.5 irradiation (100 $mW \cdot cm^{-2}$) of 2.07% were obtained for solar cells based on I2 and of 1.87% and 1.50% for I3 and I1, respectively. The open circuit voltage V_{oc} was demonstrated to be enhanced by the introduction of dodecyl or benzyl moieties on the indole groups. The nonplanar structure of bisindolylmaleimide was proven to be effective in aggregation resistance. This work suggests that organic sensitizers with maleimide as electron acceptor are promising candidates as organic sensitizers in dye-sensitized solar cells.

Keywords maleimide, dye-sensitized solar cell, organic sensitizer, nonplanar

1 Introduction

Dye-sensitized solar cell (DSSC) is a real revolution in solar energy after 40 years of the invention of silicon solar cell and has been growing and progressing by leaps and bounds [1–7]. DSSCs based on Ru dyes can produce the efficiency (η) of solar energy to electricity conversion up to 11% under amplitude modulated (AM) 1.5 irradiation [8–13]. Nowadays, many kinds of metal-free organic dyes, such as coumarin [14–19], triarylamine [20–27], indoline [28–31], hemicyanine [32–34], merocyanines [35], squaraine [36,37] benzothiadiazole [38], boradiazaindacenes [39], porphyrin [40–43], cyanine [44–48], perylene [49–52], azulene [53], and other oligothiophene dyes [54–59] are being intensively investigated because of their facile design and synthesis, convenient control of absorption wavelength and lower cost. The performance of DSSCs based on organic dyes has recently been remarkably improved; however, their efficiency, ranging from 4-9%, still lags behind the efficiency of Ru complexes. Hence, pure organic dyes with novel structures and excellent solar energy conversion performance are highly needed.

Organic sensitizers usually have a rod-like D–π–A configuration. Extension of the π linkage is an effective way to obtain desired broad spectral properties. However, this would simultaneously cause several problems in terms of complicated synthetic procedures, chemical instability, and tendency to aggregate. The dye aggregates formed on the semiconductor surface are considered to be one of the major factors accounting for the low photovoltaic performance of DSSCs based on organic dyes [60]. Aggregation may lead to intermolecular quenching or molecules residing in the system not functionally attached to the TiO_2 surface and thus acting as filters. Moreover, the close π–π aggregation may result in instability of the organic dyes because of the formation of excited triplet states and unstable radicals under light irradiation [61,62]. Consequently, in pursuit of DSSCs with optimal performance, aggregation of organic dyes needs to be avoided through rational molecular design. The adoption of a bulky conjugated donor moiety [47,48,51,63] or introduction of long alkyl chains at the π linkage [51,52,64,65] were attempts along this line in modifying the traditional rod-like D–π–A configuration in order to minimize the intermolecular π–π stacking. Nevertheless, these approaches brought about another problem of tedious synthetic procedure. We expect that the problem can be tackled by designing new dyes with shorter π linkage between the donor and acceptor while maintaining the wide absorption spectra in visible light region.

Organic chromophores with maleimide as the electron acceptor unit were effectively used as host red luminescence materials in the fabrication of organic light-emitting diodes due to their unique persistence of strong red emissions even in the solid state [66–69]. This feature is attributed to the disturbance of the π–π stacking by the nonplanar geometry of maleimide based derivatives. The disturbance could thus minimize loss through the associated deactivation of the excited state, which is also critical for the conversion efficiency of the DSSCs [70]. In addition, these derivatives exhibit broad absorption spectra in the visible region. We assume that these attractive characters of such kind of dyes could be exploited in the DSSCs. Herein we describe a series of organic sensitizers I1, I2, and I3 based on bisindolylmaleimide derivatives (see Scheme 1).

Received March 18, 2009; accepted April 8, 2009
1. Key Lab for Advance Materials and Institute of Fine Chemicals, East China University of Science and Technology, Shanghai 200237, China
2. Theoretical Chemistry, School of Biotechnology, Royal Institute of Technology, S-10691 Stockholm, Sweden
E-mail: ningzj82@163.com

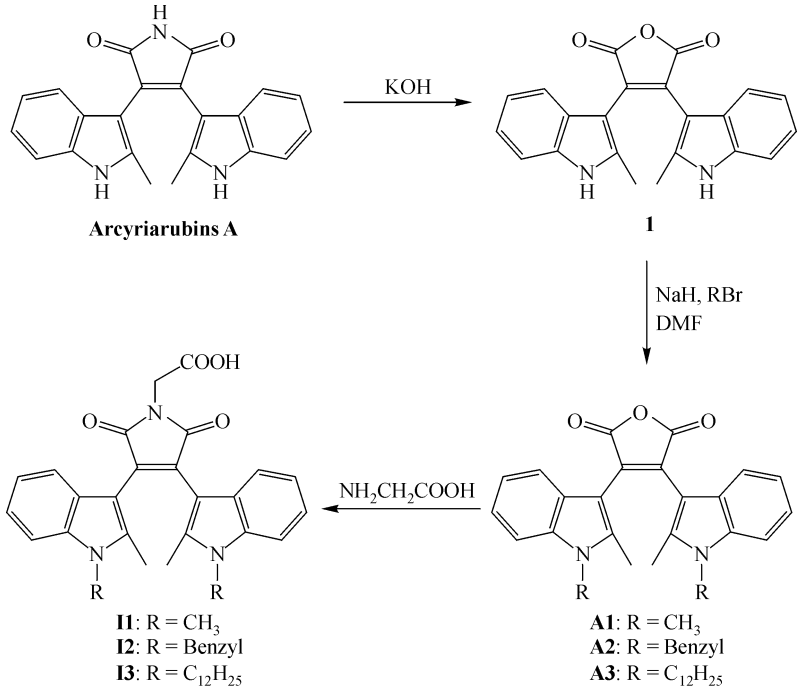

Scheme 1 Synthetic route for compounds I1, I2 and I3.

2 Experiments

2.1 Chemicals and instruments

^{1}H NMR measurements were performed on a Brücker AM 400 spectrometer. Mass spectra were acquired using a Waters Micromass LCT mass spectrometer. UV-Vis spectra were recorded on a Varian Cary 500 spectrophotometer and fluorescence emission spectra were on a Varian Cary Eclipse fluorescence spectrophotometer. Cyclic voltammetry was performed using a Potentiostat/Galvanostat Model K0264 (Princeton Applied Research). Anhydrous CH_2Cl_2 was used as solvent under inert atmosphere, and 0.1 mol/L tetra(n-butyl) ammonium hexafluorophosphate (TBAHFP) was used as the supporting electrolyte. A platinum disk electrode was used as the working electrode, a platinum wire as the counter electrode, and a saturated Ag/AgCl reference electrode. The starting material compound 1 was prepared from Arcyriarubins A according to the published procedure [66,67].

2.2 Preparation of dye-sensitized nanocrystalline TiO_2 electrodes

The dye-sensitized TiO_2 electrode was prepared according to the procedure in literature. TiO_2 colloidal dispersion was made according to reference [71] employing commercially available TiO_2 (P25, Degussa AG, Germany). Films of nanocrystalline TiO_2 colloidal on FTO glass were prepared by sliding a glass rod over the conductive side of the FTO glass. Sintering was carried out at 450°C for 30 min. Before immersion into the dye solution, these films were soaked in 0.2 mol/L aqueous $TiCl_4$ solution overnight in a closed chamber. The method was proven to increase the short-circuit photocurrent significantly [71]. The thickness of the TiO_2 film was about 12.5 μm. After being washed with deionised water and fully rinsed with ethanol, the films were heated again at 450°C followed by cooling to 80°C and dipping into a 3×10^{-4} mol/L solution of dyes in ethanol for 12 h at room temperature. The dye-coated TiO_2 film, as the working electrode, was placed on top of an FTO glass as a counter electrode, on which Pt was sputtered. The redox electrolyte was introduced into the inter-electrode space by capillary force.

2.3 Photoelectrochemical measurements

The photoelectrochemical experiments were performed in sandwich-type two-electrode cells. The dye-coated film was used as the working electrode, platinic FTO glass as the counter electrodes and 0.4 mol/L 1-methyl-3-propyl imidiazolium iodide, 0.3 mol/L LiI, and 0.03 mol/L I_2 in mixed solution of acetonitrile and 3-methyl-2-oxazolidinone (volume ratio: 9∶1) was used as electrolyte. The photocurrent action spectra were measured using a Model SR830 DSP Lock-In Amplifier and a Model SR540 Optical Chopper (Stanford Research Corporation, USA), a 7IL/PX150 xenon

lamp and power supply, and a 7ISW301 Spectrometer. The irradiation source for the photocurrent density–voltage (*J-V*) measurement is an AM 1.5 solar simulator (Newport-91160-1000). The incident light intensity was 100 $mW \cdot cm^{-2}$, calibrated with a standard silicon solar cell. The tested solar cells were masked to a working area of 0.15 cm^2. *J-V* characteristic was obtained on a Model 2400 Sourcemeter (Keithley Instruments, Inc. USA).

2.4 Synthesis

The synthetic scheme is illustrated in Scheme 1. Alkylation of compound 1 in the presence of NaH in DMF produced bisindolylmaleic anhydrides derivatives A1, A2 and A3. Subsequent imidization of A1, A2 and A3 with amino acetic acid in ethylene glycol monomethyl ether conveniently yielded the corresponding carboxyl attached bisindolylmaleimide derivatives I1, I2 and I3.

General procedure for the synthesis of A1, A2 and A3 are described as below. Deprotonation of compound 1 (1 mmol) with NaH (2 mmol) in DMF (5 mL) was followed by dropwise addition of corresponding alkyl bromide reactants (2.2 mmol). The reaction mixture was stirred at room temperature for ca. 3 h and then quenched by water. After filtration, the filtrate was purified via column chromatography (eluted with CH_2Cl_2/hexane).

2,3-Bis(N-methyl-2′methyl-3′-indolyl)maleic anhydride (A1). ^{1}H NMR ($CDCl_3$): δ: 7.23 (d, 2H, J = 8.2 Hz), 7.12 (dd, 4H, J = 7.4 Hz, 7.5 Hz), 6.91 (t, 2H, J = 7.5 Hz), 3.58 (s, 6H), 2.04 (s, 6H).

2,3-Bis (N-benzyl-2′methyl-3′-indolyl)maleic anhydride (A2). ^{1}H NMR ($CDCl_3$): δ: 7.51–7.53 (m, 2H), 7.33–7.39 (m, 2H), 7.27–7.31 (m, 2H), 7.12–7.20 (br, 8H), 6.93 (br, 2H), 6.69 (br, 2H), 5.25 (br, 4H), 2.01 (br, 6H).

2,3-Bis (N-dodecyl-2′methyl-3′-indolyl)maleic anhydride (A3). ^{1}H NMR ($CDCl_3$): δ: 7.23 (d, 2H, J = 8.2 Hz), 7.12 (dd, 4H, J = 7.4 Hz, 7.5 Hz), 6.91 (t, 2H, J = 7.5Hz), 3.99 (t, 4H, J = 6.8 Hz), 2.04 (s, 6H), 1.59 (br, 4H), 1.25–1.31 (br, 36H), 0.88 (t, 6H, J = 6.8 Hz).

General procedure for the synthesis of I1, I2 and I3 are summarized as below. To a solution of bisindolylmaleic anhydride derivative A1 (or A2 or A3) (1 mmol) in ethylene glycol monomethyl ether (10 mL), amino acetic acid (1.1 mmol) was added. The mixture was refluxed for ca. 24 h. Solvent removal by rotary evaporator was followed by purification via column chromatography (eluted with CH_2Cl_2/CH_3OH), leading to corresponding carboxyl attached bisindolylmaleimide derivative I1 (or I2 or I3).

2-(3,4-bis(1,2-dimethyl-1H-indol-3-yl)-2,5-dioxo-2H pyrrol-1(5H)-yl)acetic acid (I1) ^{1}H NMR ($CDCl_3$): 7.20 (d, 2H, J = 8.4 Hz), 7.11 (t, 4H, J = 7.6 Hz), 6.92 (br, 2H), 4.52 (s, 2H), 3.58 (s, 6H), 2.05 (s, 6H). HRMS (*m/z*): $[M]^+$ calcd. for $C_{26}H_{22}N_3O_4$,441.1689. Found: 441.1690.

2-(3,4-bis(1-benzyl-2-methyl-1H-indol-3-yl)-2,5-dioxo-2H-pyrrol-1(5H)-yl) acetic acid (I2) ^{1}H NMR ($CDCl_3$): δ: 7.11–7.19 (br, 12H), 6.90 (t, 4H, J = 6.8 Hz), 6.68 (br, 2H), 5.22 (br, 4H), 4.45 (s, 2H), 2.02 (br, 6H). HRMS (*m/z*): $[M]^+$ calcd. for $C_{38}H_{31}N_3O_4$,593.2315. Found: 593.2317.

2-(3,4-bis(1-dodecyl-2-methyl-1H-indol-3-yl)-2,5-dioxo 2H-pyrrol-1(5H)-yl) acetic acid (I3) ^{1}H NMR ($CDCl_3$): δ: 7.20 (d, 2H, J = 8.4 Hz), 7.09 (t, 4H, J = 7.6 Hz), 6.89 (br, 2H), 4.52 (s, 2H), 3.98 (br, 4H), 2.01 (s, 6H), 1.58 (br, 4H), 1.27 (s, 36H), 0.90 (t, 6H, J = 6.8 Hz). HRMS (*m/z*): $[M]^+$ calcd. for $C_{48}H_{67}N_3O_4$,749.5132. Found: 749.5134.

3 Results and discussion

3.1 Absorption and emission spectra and electrochemical properties of the dyes

The absorption and emission spectra of I1, I2 and I3 in dilute solution of CH_2Cl_2 are shown in Figure 1. Their photophysical parameters are presented in Table 1. In CH_2Cl_2, I1, I2 and I3 exhibit similar broad absorption bands in the visible

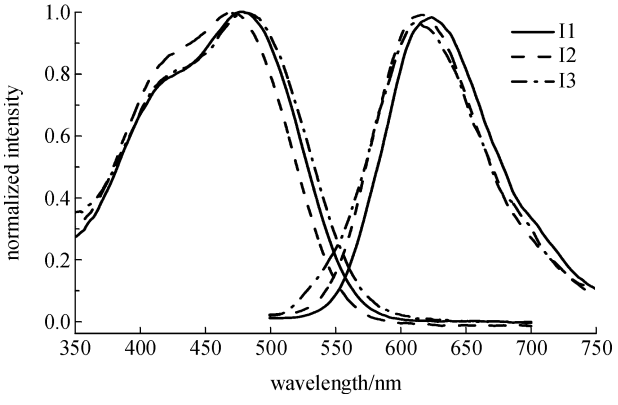

Figure 1 Normalized absorption (left) and emission (right) spectra of dyes in CH_2Cl_2 (1×10^{-5} mol/L).

Table 1 Optical and electrochemical properties of the dyes

dye	λ_{max}[a] [nm] [$\varepsilon\times10^4$(mol/L)$^{-1}$cm^{-1}]	λ_{em}[b] [nm]	E_{0-0}[c] [eV]	HOMO [eV]	LUMO [eV]
I1	477 (0.709), 421 (0.558)	626	2.26	−5.34	−3.08
I2	469 (0.634), 422 (0.542)	614	2.30	−5.44	−3.14
I3	480 (0.684), 420 (0.551)	620	2.32	−5.36	−3.04

a Absorption maximum in CH_2Cl_2; b Emission maximum of the dyes in CH_2Cl_2, I1, I2 and I3 are excited at absorption maximum, respectively. c The zeroth-zeroth transition E_{0-0} value was estimated from the intersection of the absorption and emission spectra.

region from 350 to 580 nm with shoulders at around 420 nm. The absorption maxima of I1 and I3 sensitizers, which have alkyl chains attached to nitrogens in indole groups, are located at 477 and 480 nm, respectively. In comparison, I2, which bears benzyl substituents at nitrogens instead, displays blue-shifted absorption maximum by about 10 nm. Upon irradiating with the maximum absorption wavelength, I1, I2 and I3 show red luminescence at 624, 615 and 612 nm, respectively.

To evaluate the possibility of electron transfer from the excited dye molecules to the conductive band of TiO_2, cyclic voltammograms were performed in CH_2Cl_2 solution. Each compound displays two redox processes (Figure 2), which are due to the oxidations of the two indole units in the donor moieties. The reversible nature of these peaks indicates the electrochemical stability of the dyes. Dyes with good redox stability are required for sustaining DSSCs. The half-peak potentials ($E_{1/2}$)= 1/2(E_{pa} + E_{pc}) of the first oxidation wave were estimated to be 1.04, 1.14 and 1.06 V for I1, I2 and I3, respectively. The highest occupied molecular orbital (HOMO) and the lowest unoccupied molecular orbital (LUMO) levels derived from the oxidation potentials and UV-vis absorption data of these dyes are summarized in Table 1. The HOMOs are sufficiently low in energy compared to I^-/I_3^- redox couple, hence facilitating efficient dye regeneration. Judging from the LUMO value, the excited-state energy levels for the dyes are much higher than the bottom of the conduction band of TiO_2 (−4.4 eV), indicating that the electron injection process from the excited dye molecule to TiO_2 conduction band is energetically favorable.

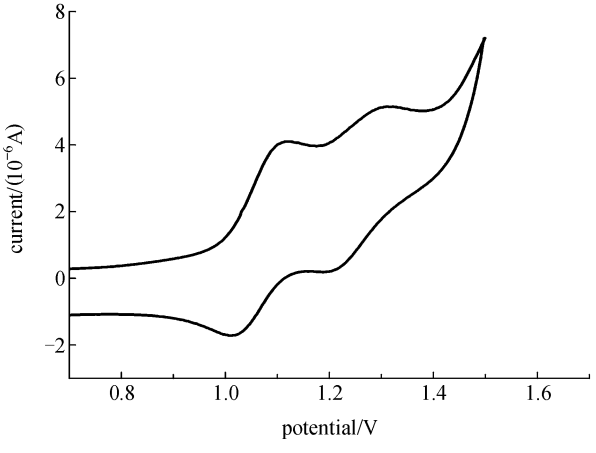

Figure 2 Oxidative cyclic voltammogram of I3 measured in CH_2Cl_2.

3.2 Quantum chemistry calculation

The geometrical and electronic properties of I1 and I2 were studied with density functional theory (DFT) using the Gaussian 03 program package [72]. In comparison to I1, long alkyl chain substitution in I3 has negligible effect on electronic and optical properties at a molecular level, thus calculations were limited to I1 and I2. The calculations were done on a B3LYP/6-31G(d) level for geometry optimizations in the ground state. B3LYP is a hybrid function modified from the three-parameter exchange-correlation functional of Becke [73], while the gradient-corrected exchange and correlation functions are calculated according to Becke [74] and Lee *et al*. [75]. The vertical excitations were calculated by time-dependent DFT (TDDFT) with B3LYP/6-31 + G(d) in gas phase.

Table 2 Calculated TDDFT vertical excitation energies for the lowest transitions, oscillator strengths (*f*) and composition in terms of molecular orbital contributions

dye	*E*[eV]	λ[nm]	*f*	composition
I1-ap2	2.34	529	0.1415	87% HOMO→LUMO
	2.74	452	0.0757	90% HOMO-1→LUMO
I2-ap2	2.37	522	0.1274	88% HOMO→LUMO
	2.73	454	0.0787	91% HOMO-1→LUMO

For I1 and I2, three different stable structures are located, namely parallel (p) and anti-parallel (ap1 and ap2) conformers. Figure 3 and Table 3 show the details of the different conformers. In the anti-parallel conformers, the two indole groups are both aligned in pseudo-*E* geometry (ap1) or pseudo-*Z* geometry (ap2) with respect to the maleimide. In the parallel (p) conformer, the two indole groups are oriented in different fashions, i.e., one in pseudo-*E* geometry and the other in pseudo-*Z* geometry. For both I1 and I2, due to the steric repulsion between the two indole groups, the ap2 conformers were calculated to be most stable and ap1 conformers most unstable. This result complies with the single crystals of analogous structures [69]. Hence, ap2 conformers were chosen as the conformations used in the theoretical comparison.

Table 3 Relative energies and dihedral angle parameters for the parallel (p) and anti-parallel (ap) conformers of I1 and I2

dye	relative energy (kcal·mol^{-1})	$\lvert C_{a'}-C_a-C_b-C_c\rvert$	$\lvert C_a-C_{a'}-C_{b'}-C_{c'}\rvert$
I1-p	0.42	−45.05	139.58
I1-ap1	1.20	47.18	47.77
I1-ap2	0	139.85	140.35
I2-p	0.45	−42.22	143.27
I2-ap1	2.55	44.42	44.48
I2-ap2	0	141.57	142.28

Figure 4 depicts the optimized ground state geometries and isodensity plots of the frontier molecular orbitals for I1 and I2. This figure and the listed structural parameters in Table 3 clearly show the nonplanar configuration of these

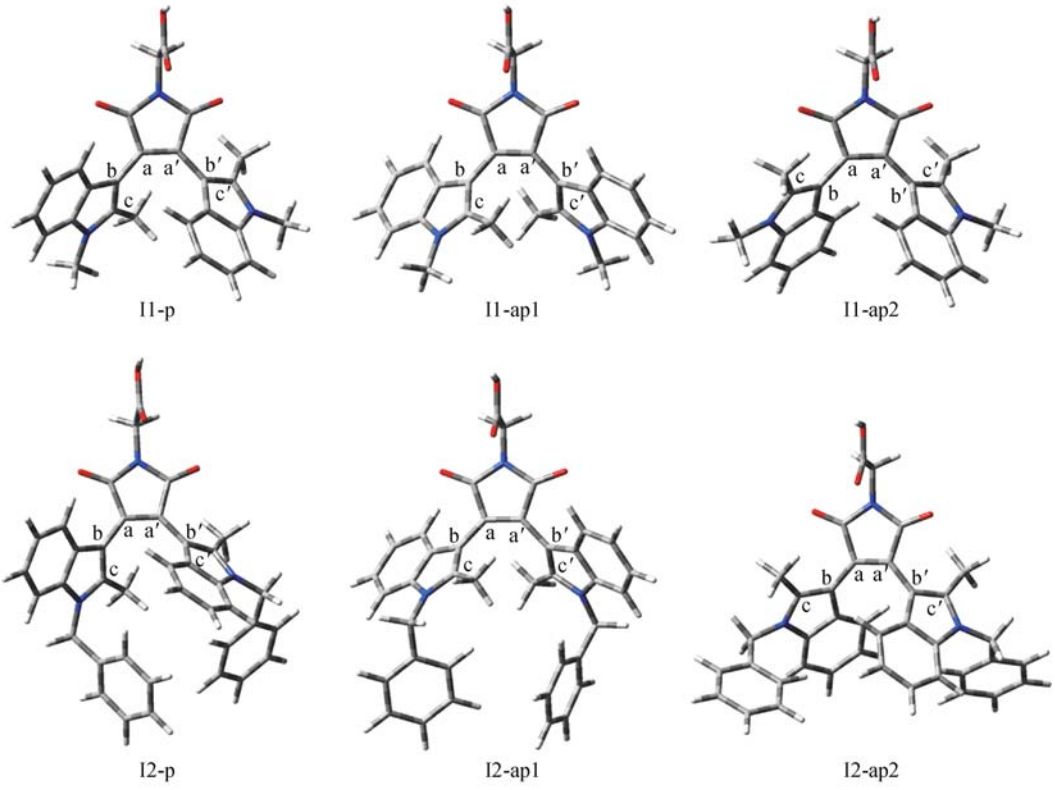

Figure 3 Optimized structures obtained without symmetry constraint for the parallel (p) and anti-parallel (ap) conformers of I1 and I2 using the B3LYP/6-31G basis.

bisindolylmaleimide derivatives. In these two molecules, the HOMO and HOMO-1 are π bonding orbitals distributed over the indole groups and the maleimide moiety; the LUMO is a π* orbital localized in the maleimide moiety. As can be seen in Table 2, for I1 and I2, the lowest singlet-singlet excitation energy is calculated at 2.34 and 2.37 eV, respectively. This blue shift of the absorption maximum for I2 is in accordance with the experiment. The lowest transition corresponds to a HOMO→LUMO transition, accompanied by a pronounced intramolecular charge transfer from the whole molecule to the maleimide moiety. However, there is little electron density on the carboxylic group, which may affect the quantum yield of charge injection due to the weak electronic coupling between the dye excited state and the TiO_2 conduction band. The next transition originates from the HOMO-1→LUMO transition and is responsible for the shoulder peak in the absorption spectra. The TDDFT excitation energies are in qualitative agreement with the experimentally observed spectroscopic behavior of I1 and I2, but the absorption maxima are greatly underestimated. This is related to the extended charge-transfer character of this transition, which is not properly captured by TDDFT calculations employing the current exchange-correlation functional [76].

3.3 Cell performance

The incident photon-to-current conversion efficiencies (IPCE) and *J-V* characteristics of devices based on these dyes are illustrated in Figures 5 and Figure 6, respectively. The photoelectrochemical properties of dyes sensitized TiO_2 electrodes are tabulated in Table 4. In general, the IPCE data of these dyes exhibit a moderate efficiency of 42%–52%, which may be ascribed to the relatively low quantum yield of charge injection as mentioned above. The IPCE spectra are consistent with their absorption spectra in solution, meaning that there is no distinct aggregation of the sensitizers on the TiO_2 surface [25–27, 63]. I2 has the highest short-circuit current (J_{sc}) of 7.84 mA·cm^{-2}, while I1 exhibits the lowest current value of 6.63 mA·cm^{-2}. Meanwhile, the open-circuit voltage (V_{oc}) of I2 (426 mV) and I3 (432 mV) are higher than that of I1 (391 mV) in the same condition. In I2 and I3, the charge recombination process may be restrained to some extent due to the isolation effect of the long alkyl chains and the benzyl groups, which can block the approach of the redox couple to the TiO_2 surface. The low J_{sc} of I3 may be caused by its relatively low adsorption dye amount. Overall, the maximum η value of 2.07% (J_{sc} = 7.84 mA·cm^{-2}, V_{oc} =

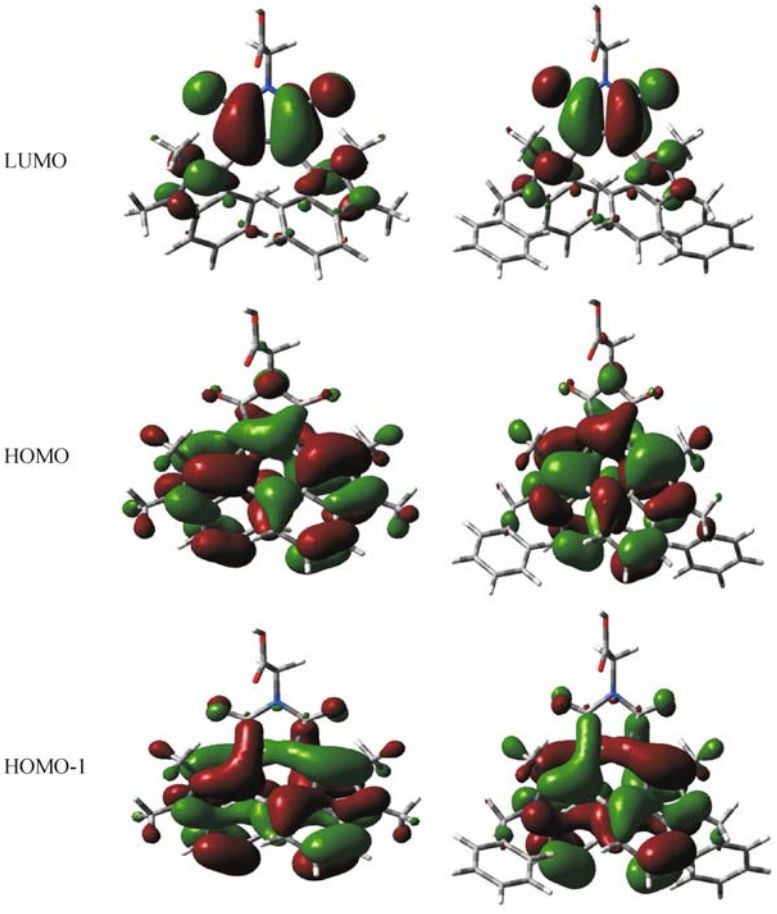

Figure 4 Optimized ground state geometries and isodensity surface plots of HOMO-1, HOMO and LUMO of I1-ap2 and I2-ap2.

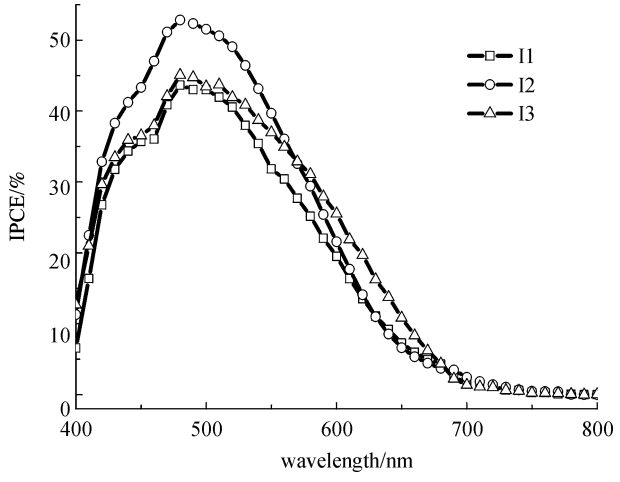

Figure 5 Action spectra of monochromatic incident photon-to-current conversion efficiency for DSSCs based on I1, I2 and I3.

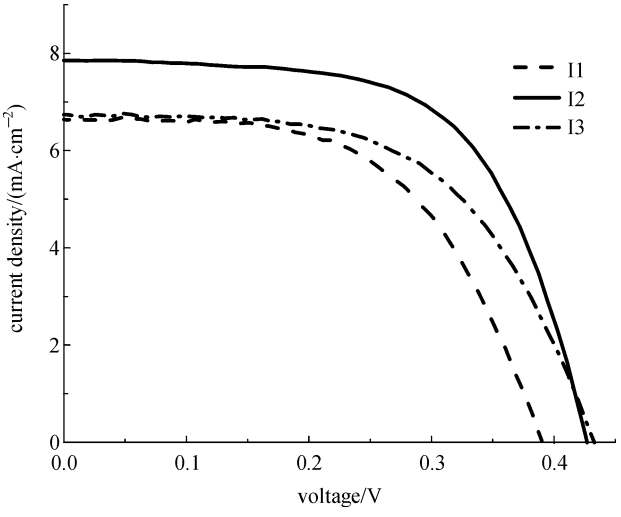

Figure 6 Photocurrent-voltage curves for DSSCs based on I1, I2 and I3.

426 mV, and fill factor (*FF*) = 0.62) was achieved using a DSSC based on I2.

Additionally, a comparison between the cells with and without the addition of deoxycholic acid (DCA), which is commonly applied in coadsorption to prevent charge recombination, has been carried out [60]. As shown in

Table 4 Photovoltaic performance of DSSCs based on I1, I2 and I3, compared to the N719 dyes

dye	J_{sc} ($mA \cdot cm^{-2}$)	V_{oc} (mV)	fill factor (*FF*)	η (%)	amount[a]/10^{-7} $mol \cdot cm^{-2}$
I1	6.63	391	0.58	1.50	2.8
DCA-I1	8.12	430	0.60	2.09	
I2	7.84	426	0.62	2.07	2.4
DCA-I2	7.42	427	0.61	1.93	
I3	6.75	432	0.64	1.87	2.2
DCA-I3	6.77	433	0.62	1.82	
N179	17.6	597	0.62	6.51	

a Amount of the dyes adsorbed on TiO_2 film.

Figure 7, the addition of DCA had little effect on the overall performance of DSSC based on I2, whereas the photocurrent is decreased due to the lower dye adsorption amount, suggesting that the charge recombination process might have already been restrained to some extent because of the isolation effect of the long alkyl chains and the benzyl groups. On the contrary, the J_{sc}, V_{oc} and the overall performance of DSSC based on I1 have been improved for the reduction of the charge recombination upon the addition of DCA.

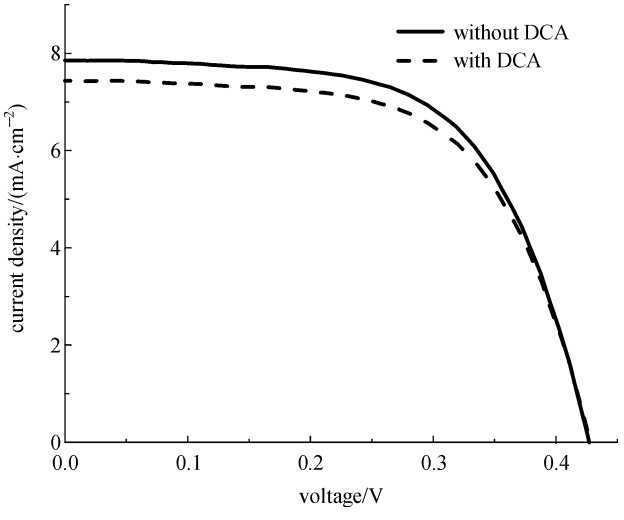

Figure 7 Photocurrent-voltage curves for DSSCs based on I2 with (dashed line) and without (solid line) the addition of DCA (1×10^{-3} mol/L) to the dye bath.

4 Conclusion

In this study, three bisindolylmaleimide derivatives (I1, I2 and I3), where maleimide groups served as electron acceptor, were synthesized and investigated as sensitizers for the application in nanocrystalline TiO_2 solar cells. The maximum conversion efficiency reaches 2.09% under AM 1.5 illumination. This value has the potential to be enhanced by transforming the electron donor group. For I2 and I3 dyes, it was found that the introduction of dodecyl or benzyl moieties on the indole groups contributed to the enhanced V_{oc} by impeding the approach of I_3^- ions to the TiO_2 surface. Quantum chemistry calculations confirmed the nonplanar geometry of these dyes. The calculation also revealed that the weak electronic coupling between the dye excited state and the TiO_2 conduction band might affect the quantum yield of charge injection, responsible for the moderate IPCEs.

Acknowledgements The authors thank Prof. He Tian in the Key Lab for Advance Materials and Institute of Fine Chemicals, East China University of Science and Technology, Shanghai for supervision. The authors are grateful to Dr. Yaoquan Tu and Prof. Hans Ågren in the Department of Theoretical Chemistry at the Royal Institute of Technology in Sweden for computational assistance. This work was supported by the National Natural Science Foundation of China (Grant No. 50673025), the National Basic Research Program of China (No. 2006CB806200) and Scientific Committee of Shanghai.

References

1. O'Regan, B.; Gratzel, M., *Nature* **1991**, *353*, 737
2. Gao, F.; Wang, Y.; Shi, D.; Zhang, J.; Wang, M.; Jing, X.; Humphry-Baker, R.; Wang, P.; Zakeeruddin, S. M.; Grätzel, M., *J. Am. Chem. Soc*. **2008**, *130*, 10720
3. Zhao, Y.; Zhai, J.; He, J. L.; Chen, X.; Chen, L.; Zhang, L. B.; Tian, Y. X.; Jiang, L.; Zhu, D. B., *Chem. Mater*. **2008**, *20*, 6022
4. Robertson, N., *Angew. Chem. Int. Ed*. **2006**, *45*, 2338
5. Snaith, H. J.; Schmidt-Mende, L., *Adv. Mater*. **2007**, *19*, 3187
6. Chen, Z. G.; Yang, H.; Li, X. H.; Li, F. Y.; Yi, T.; Huang, C. H., *J. Mater. Chem.* **2007**, *17*, 1602
7. Yang, H.; Yu, C. Z.; Song, Q. L.; Xia, Y. Y.; Li, F.; Chen, Z. G.; Li, X. H.; Yi, T.; Huang, C. H., *Chem. Mater*. **2006**, *18*, 5173
8. Kuang, D. B.; Ito, S.; Wenger, B.; Klein, C.; Moser, J.; Humphry-Baker, R.; Zakeeruddin, S. M.; and Grätzel, M., *J. Am. Chem. Soc*. **2008**, *128*, 10720
9. Lopez-Luke, T.; Wolcott, A.; Xu, L. P.; Chen, S. W.; Wen, Z. H.; Li, J. H.; Zhang, J. Z., *J. Phys. Chem. C* **2008**, *112*, 1282
10. Hagfeldt, A.; Grätzel, M., *Acc. Chem. Res*. **2000**, *33*, 269
11. Islam, A.; Chowdhury, F. A.; Chiba, Y.; Komiya, R.; Fuke, N.; Ikeda, N.; Nozaki, K.; Han, L., *Chem. Mater*. **2006**, *18*, 5178
12. Wang, Z. S.; Kawauchi, H.; Kashima, T.; Arakawa, H., *Coord. Chem. Rev*. **2004**, *248*, 1381
13. Yam, V. W-W.; Lo, K. K-W., *Coord. Chem. Rev*. **1999**, *184*, 157
14. Hara, K.; Sayama, K.; Ohga, Y.; Shinpo, A.; Suga, S.; Arakawa, H., *Chem. Commun*. **2001**, *6*, 569
15. Hara, K.; Sato, T.; Katoh, R.; Furube, A.; Ohga, Y.; Shinpo, A.; Suga, S.; Sayama, K.; Sugihara, H.; Arakawa, H., *J. Phys. Chem. B*. **2003**, *107*, 597
16. Wang, Z, S.; Cui, Y.; Hara, K.; Dan-oh, Y.; Kasada, C.; Shinpo, A., *Adv. Mater*. **2007**, *19*, 1138
17. Hara, K.; Kurashige, M.; Dan-oh, Y.; Kasada, C.; Shinpo, A.; Suga, S.; Sayama, K.; Arakawa, H., *New J. Chem*. **2003**, *27*, 783

18. Wang, Z.; Cui, Y.; Dan-oh, Y.; Kasada, C.; Shinpo, A.; Hara, K., *J. Phys. Chem. C* **2007**, *111*, 7224
19. Hara, K.; Wang, Z.; Sato, T.; Furube, A.; Katoh, R.; Sugihara, H.; Dan-oh, Y.; Kasada, C.; Shinpo, A.; Suga, S., *J. Phys. Chem. B* **2005**, *109*, 15476
20. Hagberg, D. P.; Edvinsson, T.; Marinado, T.; Boschloo, G.; Hagfeldt, A.; Sun, L., *Chem. Commun*. **2006**, *21*, 2245
21. Hagberg, D. P.; Yum, J. H.; Lee, H.; De Angelis, F.; Marinado, T.; Karlsson, K. M.; Humphry-Baker, R.; Sun, L.; Hagfeldt, A.; Grätzel, M.; Nazeeruddin, Md. K., *J. Am. Chem. Soc*. **2008**, *130*, 6259
22. Kim, S.; Lee, J. K.; Kang, S. O.; Ko, J.; Yum, J. H.; Fantacci, S.; De Angelis, F.; DiCenso, D.; Nazeeruddin, Md. K.; Grätzel, M., *J. Am. Chem. Soc*. **2006**, *128*, 16701
23. Liang, M.; Xu, W.; Cai, F.; Chen, P.; Peng, B.; Chen, J.; Li, Z. J., *Phys. Chem. C* **2007**, *111*, 4465
24. Zhou, G.; Pschirer, N.; Schöneboom, J. C.; Eickemeyer, F.; Baumgarten, M.; Müllen, K., *Chem. Mater*. **2008**, *20*, 1808
25. Qin, P.; Yang, X.; Chen, R.; Sun, L.; Marinado, T.; Edvinsson, T.; Boschloo, G.; Hagfeldt, A., *J. Phys. Chem. C* **2007**, *111*, 1853
26. Hagberg, D. P.; Marinado, T.; Karlsson, K. M.; Nonomura, K.; Qin, P.; Boschloo, G.; Brinck, T.; Hagfeldt, A.; Sun, L., *J. Org. Chem.***2007**, *72*, 9550
27. Justin Thomas, K. R.; Hsu, Y. C.; Lin, J. T.; Lee, K. M., *Chem. Mater*. **2008**, *20*, 1830
28. Horiuchi, T.; Miura, H.; Uchida, S., *Chem. Commun*. **2003**, *24*, 3036
29. Horiuchi, T.; Miura, H.; Sumioka, K.; Uchida, S., *J. Am. Chem. Soc*. **2004**, *126*, 12218
30. Ito, S.; Zakeeruddin, S. M.; Humphry-Baker, R.; Liska, P.; Charvet, R.; Comte, P.; Nazeeruddin, M. K.; Péchy, P.; Takata, M.; Miura, H.; Uchida, S.; Grätzel, M., *Adv. Mater*. **2006**, *18*, 1202
31. Dentani, T.; Kubota, Y.; Funabiki, K.; Jin, J.; Yoshida, T.; Minoura, H.; Miurad, H.; Matsui M., *New J. Chem*. **2009**, *33*, 93
32. Wang, Z. S.; Li, F. Y.; Huang, C. H., *Chem. Commun*. **2000**, *20*, 2063
33. Chen, Y. S.; Chao, L.; Zeng, Z. H.; Wang, W. B.; Wang, X. S.; Zhang, B. W., *J. Mater. Chem.***2005**, *15*, 1654
34. Yao, Q. H.; Meng, F. S.; Li, F. Y.; Tian, H.; Huang, C. H., *J. Mater. Chem*. **2003**, *13*, 1048
35. Sayama, K.; Hara, K.; Mori, N.; Satsuki, M.; Suga, S.; Tsukagoshi, S.; Abe, Y.; Sugihara, H.; Arakawa, H., *Chem. Commun*. **2000**, *13*, 1173
36. Tatay, S.; Haque, S. A.; O'Regan, B.; Durrant, J. R.; Verhees, W. J. H.; Kroon, J. M.; Vidal-Ferran, A.; Gaviña, P.; Palomares, E., *J. Mater. Chem.***2007**, *17*, 3037
37. Matsui, M.; Nagasaka, K.; Tokunaga, S.; Funabiki, K.; Yoshida, T., *Dyes and Pigments* **2003**, *58*, 219
38. Velusamy, M.; Justin Thomas, K. R.; Lin, J. T.; Hsu, Y. C.; Ho, K. C., *Org. Lett*. **2005**, *7*, 1899
39. Erten-Ela, S.; Yilmaz, M. D.; Icli, B.; Dede, Y.; Icli, S.; Akkaya, E. U., *Org. Lett*. **2008**, *10*, 3299
40. Wang, Q.; Campbell, W. M.; Bonfantani, E. E.; Jolley, K. W.; Officer, D. L.; Walsh, P. J.; Gordon, K.; Humphry-Baker, R.; Nazeeruddin, M. K.; Grätzel, M., *J. Phys. Chem. B* **2005**, *109*, 15397
41. Eu, S.; Hayashi, S.; Umeyama, T.; Matano, Y.; Araki, Y., *J. Phys. Chem. C* **2008**, *112*, 4396
42. He, J.; Benkö, G.; Korodi, F.; Polívka, T.; Lomoth, R.; Åkermark, B.; Sun, L.; Hagfeldt, A.; Sundström, V., *J. Am. Chem. Soc*. **2002**, *124*, 4922
43. O'Regan, B. C.; López-Duarte, I.; Martínez-Díaz, M. V.; Forneli, A.; Albero, J.; Morandeira, A.; Palomares, E.; Torres, T.; Durrant, J. R., *J. Am. Chem. Soc.* **2008**, *130*, 2906
44. Zhan, W. H.; Wu, W. J.; Hua, J. L.; Jing, Y. H.; Meng, F. S.; Tian, H., *Tetra. Lett.* **2007**, *48*, 2461
45. Meng, F. S.; Yao, Q. H.; Shen, J. G.; Li, F. L.; Huang, C. H.; Chen, K. C.; Tian, H., *Synth. Met*. **2003**, *137*, 1543
46. Guo, M.; Diao, P.; Ren, Y. J.; Meng, F. S.; Tian, H.; Cai, S. M., *Sol. Energy Mater. Sol. Cells* **2005**, *88*, 23
47. Chen, X. Y.; Guo, J. H.; Peng, X. J.; Guo, M.; Xu, Y. Q.; Shi, L.; Liang, C. L.; Wang, L.; Gao, Y. L.; Sun, S. G.; Cai, S. M., *J. Photochem. Photobiol. A*, **2005**, *171*, 231
48. Ma, X. M.; Hua, J. L.; Wu, W. J.; Jing, Y. H.; Meng, F. S.; Tian, H., *Tetrahedron* **2008**, *64*, 345
49. Ferrere, S.; Zaban, A.; Gregg, B. A., *J. Phys. Chem. B* **1997**, *101*, 4490
50. Tian, H.; Liu, P. H.; Zhu, W. H.; Gao, E.; Wu, D. J.; Cai, S. M., *J. Mater. Chem*. **2000**, *10*, 2708
51. Edvinsson, T.; Li, C.; Pschirer, N.; Schneboom, J.; Eickemeyer, F.; Sens, R.; Boschloo, G.; Herrmann, A.; Müllen, K.; Hagfeldt, A., *J. Phys. Chem. C* **2007**, *111*, 15137
52. Ferrere, S.; Gregg, B. A., *New J. Chem*. **2002**, *26*, 1155
53. Zhang, X. H.; Li, C.; Wang, W. B.; Cheng, X. X.; Wang, X. S.; Zhang, B. W., *J. Mater. Chem*. **2007**, *17*, 642
54. Tan, S. X.; Zhai, J.; Fang, H. J.; Jiu, T. G.; Ge, J.; Li, Y. L.; Jiang, L.; Zhu, D. B., *Eur. J.* **2005**, *11*, 6272
55. Wang, Z. S.; Koumura, N.; Cui, Y.; Takahashi, M.; Sekiguchi, H.; Mori, A.; Kubo, T.; Furube, A.; Hara, K., *Chem. Mater*. **2008**, *20*, 3993
56. Li, S. L.; Jiang, K. J.; Shao, K. F.; Yang, L. M., *Chem. Commun*. **2006**, *26*, 2792
57. Yen, Y.; Hsu, Y.; Lin, J. T.; Chang, C.; Hsu, C.; Yin, D., *J. Phys. Chem. B* **2008**, *112*, 12557
58. Chen, R. K.; Yang, X. C.; Tian, H. N.; Wang, X. N.; Hagfeldt, A.; Sun, L., *Chem. Mater*. **2007**, *19*, 4007
59. Tsai M.; Hsu Y.; Lin J T.; Chen H.; Hsu C., *J. Phys. Chem. C* **2007**, *111*, 18785
60. Hara, K.; Dan-oh, Y.; Kasada, C.; Ohga, Y.; Shinpo, A.; Suga, S.; Sayama, K., *Langmuir* **2004**, *20*, 4205
61. Liu, D.; Fessenden, R. W.; Hug, G. L.; Kamat, P. V., *J. Phys. Chem. B* **1997**, *101*, 2583
62. Fink, R. F.; Seibt, J.; Engel, V.; Renz, M.; Kaupp, M.; Lochbrunner, S.; Zhao, H. M.; Pfister, J.; Würthner, F.; Engels, B., *J. Am. Chem. Soc.* **2008**, *130*, 12858
63. Ning, Z. J.; Zhang, Q.; Wu, W. J.; Pei, H. C.; Liu, B.; Tian, H., *J. Org. Chem.* **2008**, *73*, 3791
64. Koumura, N.; Wang, Z. S.; Mori, S.; Miyashita, M.; Suzuki, E.; Hara, K., *J. Am. Chem. Soc.* **2006**, *128*, 14256

65. Kroeze, J. E.; Hirata, N.; Koops, S.; Nazeeruddin, Md. K.; Schmidt-Mende, L.; Grätzel, M.; Durrant, J. R., *J. Am. Chem. Soc*. **2006**, *128*, 16376
66. Yeh, T. S.; Chow, T. J.; Tsai, S. H.; Chiu, C. W.; Zhao, C. X., *Chem. Mater*. **2006**, *18*, 832
67. Wu, W. C.; Yeh, H. C.; Chan, L. H.; Chen, C. T., *Adv. Mater.* **2002**, *14*, 1072
68. Chiu, C. W.; Chow, T. J.; Chuen, C. H.; Lin, H. M.; Tao, Y. T., *Chem. Mater*. **2003**, *15*, 4527
69. Ning, Z. J.; Zhou, Y. C.; Zhang, Q.; Ma, D. G.; Zhang, J. J.; Tian, H., *J. Photochem. Photobiol. A: Chem*. **2007**, *192*, 8
70. Chen, R.; Yang, X.; Tian, H.; Sun, L., *J. Photochem. Photobiol. A: Chem*. **2007**, *189*, 295
71. Nazeeruddin, M. K.; Kay, A.; Rodicio, I.; Humphry-Baker, R.; Grätzel, M., *J. Am. Chem. Soc*. **1993**, *115*, 6382
72. Frisch, M. J.; Trucks, G. W.; Schlegel, H. B.; Gill, P. M. W.; Johnson, B. G.; Robb, M. A.; Cheeseman, J. R.; Keith, T.; Petersson, G. A.; Montgomery, J. A.; Raghavachari, K.; Al-Laham, M. A.; Zakrzewski, V. G.; Ortiz, J. V.; Foresman, J. B.; Cioslowski, J.; Stefanov, B. B.; Nanayakkara, A.; Challacombe, M.; Peng, C. Y.; Ayala, P. Y.; Chen, W.; Wong, M. W.; Andres, J. L.; Replogle, E. S.; Gomperts, R.; Martin, R. L.; Fox, D. J.; Binkley, J. S.; Defrees, D. J.; Baker, J.; Stewart, J. P.; Head-Gordon, M.; Gonzalez, C.; Pople, J. A., Gaussian 03, revision C.01., Gaussian.; Inc.: Pittsburgh, PA, 2004
73. Becke, A. D., *J. Chem. Phys*. **1993**, *98*, 5648
74. Becke, A. D., *J. Chem. Phys*. **1992**, *96*, 2155
75. Lee, C.; Yang, W.; Parr, R. G., *Phys. Rev. B* **1988**, *37*, 785
76. Dreuw, A.; Head-Gordon, M., *J. Am. Chem. Soc.* **2004**, *126*, 4007